Pergamon

Tetrahedron 58 (2002) 3401–3407

TETRAHEDRON

The nature of the *thermodynamically controlled* deracemization of 2-benzylcyclohexanone using (*R*,*R*)-(−)-*trans*-2,3-bis(hydroxydiphenylmethyl)-1,4-dioxaspiro[5.4]decane: a crystallographic result of inclusion complex

Hiroto Kaku, Shigeru Takaoka and Tetsuto Tsunoda*

Faculty of Pharmaceutical Sciences, Tokushima Bunri University, Tokushima 770-8514, Japan

Received 21 December 2001; accepted 4 March 2002

Abstract—An X-ray crystallographic study elucidated the structure of the inclusion complex TADDOL **1**·(*R*)-2-benzylcyclohexanone (**2**). The study disclosed that the assembly of the host molecule **1** ingeniously includes the guest molecule (*R*)-**2** via hydrogen bonding and van der Waals contacts.

1. Introduction

In previous papers, we described the *thermodynamically controlled* deracemization[1,2] of several cyclohexanones using (*R*,*R*)-(−)-*trans*-2,3-bis(hydroxydiphenylmethyl)-1,4-dioxaspiro[5.4]decane (TADDOL **1**)[3] in basic suspension media. For example, use of **1** (1.0–2.0 equiv.) with alkaline in aqueous MeOH converted racemic 2-benzylcyclohexanone (**2**) and 2-(2-methoxyethyl)cyclohexanone (**3**) to the *R*-isomer of 74 and 94% ee in quantitative yield, respectively (Scheme 1).

These unique phenomena were accomplished according to the following concept. The system functions efficiently between two phases that consist of the solid phase of powdered optically active host molecule and the liquid phase of aqueous basic MeOH, into which free guest molecule (α-monosubstituted cyclohexanones) can be solvated to some extent (Scheme 2). If the guest molecule is congenial with the host molecule, it is included into the cavity constituted by aggregation of the optically active host molecule. Therefore, the situation of the guest molecule is differentiated in three stages. Two of the stages include a

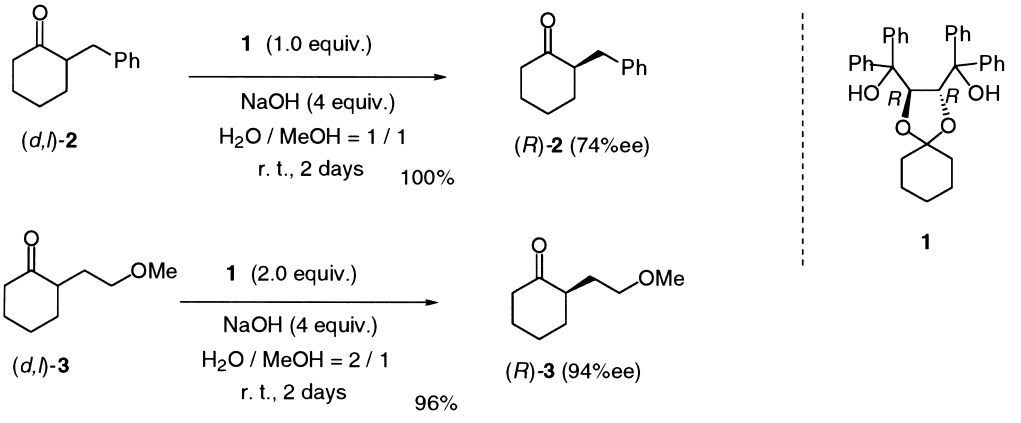

Scheme 1. Deracemization of cyclohexanones utilizing TADDOL **1**.

Keywords: deracemization; molecular recognition; inclusion; X-ray crystal structures.
* Corresponding author. Tel.: +81-88-622-9611; fax: +81-88-655-3051; e-mail: tsunoda@ph.bunri-u.ac.jp

0040–4020/02/$ - see front matter
PII: S0040-4020(02)00281-8

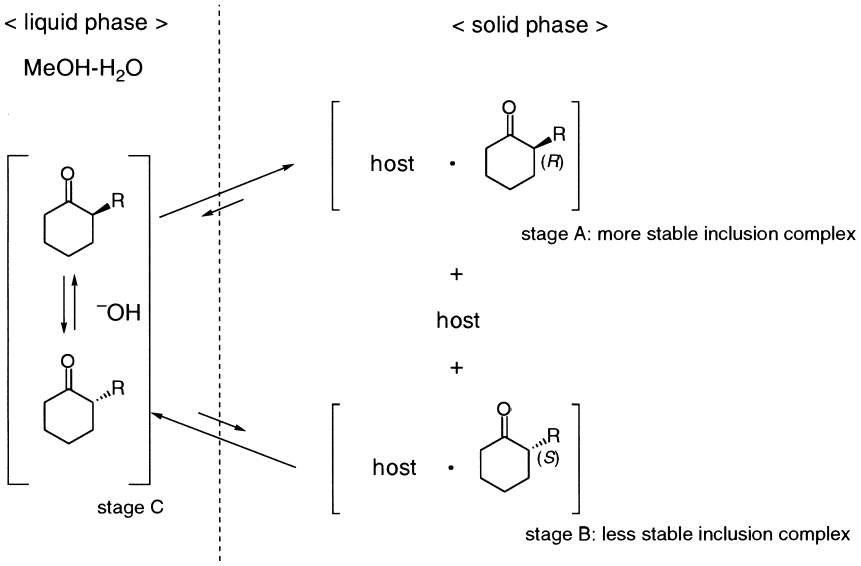

Scheme 2. Concept of deracemization.

guest molecule as the diastereomeric inclusion complex (stages A and B in Scheme 2) and one stage has a free guest molecule in the liquid phase (stage C). Since both enantiomers of the guest molecule racemize to each other in the basic liquid phase, an equilibration can arise between stages A and B via stage C. When stage A is thermodynamically more stable than stages B and C, one enantiomer of the guest molecule is enriched and recovered from the resulting mixture in excellent yield.

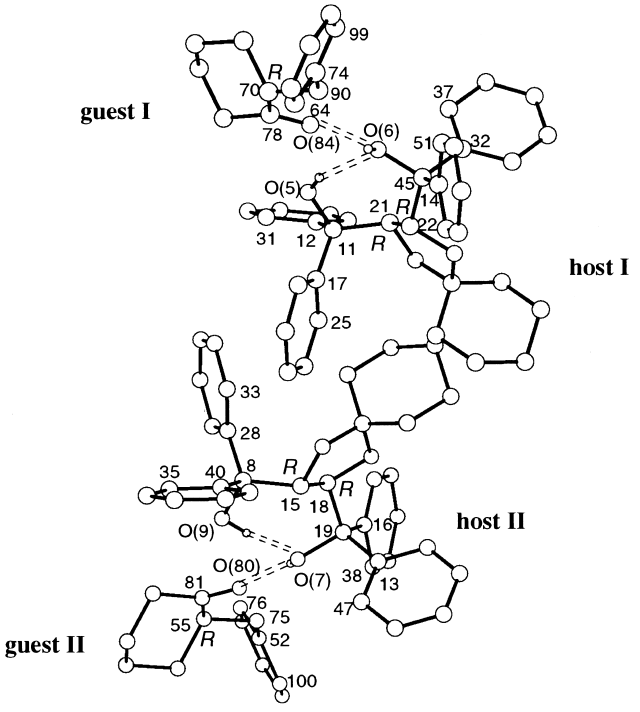

Figure 1. Molecular structure of 2:2 complex of **1** and (*R*)-**2**. Hydrogen bonds are represented by double dashed lines. The guest molecule I and II are shown after transformation to ($x-1$, y, z) and ($x+1$, y, z), respectively.

Thus, the study disclosed that deracemization based on inclusion chemistry could provide a convenient and excellent method for the preparation of optically active α-substituted cyclohexanones. However, the nature of the molecular recognition process was unclear. In this paper, we would like to describe the full details of the efficient chiral molecular recognition process disclosed by X-ray analytical studies of the **1**·(*R*)-**2** complex.

2. Results and discussion

2.1. Molecular structure of the complex 1·(*R*)-2 elucidated by X-ray crystallography

Fig. 1 illustrates the molecular structure of the complex **1**·(*R*)-**2** packed in the asymmetric unit with the atomic numbering. Two molecules of each substance **1** and (*R*)-**2** are observed in the asymmetric unit. Selected bond lengths and angles of the two independent host molecules **1** are listed in Table 1 for comparison. These values in Table 1 are normal and require no discussion. The Table also indicates that the conformational differences are not very large between the two independent host molecules, the host I and the host II. Furthermore, the TADDOL **1** keeps the propeller-like structure again, as Seebach discussed recently.[4]

Table 2 lists the same geometric parameters of the two independent guest molecules (*R*)-**2**. Furthermore, the conformational profile of **2** was examined by 4500 step Monte Carlo (MCMM) searches[5] with the MM2* force field in MacroModel®[6,7] using the GB/SA $CHCl_3$ solvent continuum model.[8,9] The most stable conformation obtained is shown in Table 2 and Fig. 2. Table 2 clearly shows

Table 1. Selected bond lengths (Å) and angles (°) for **1**

Host I		Host II	
Bond lengths (Å)			
C(11)–C(21)	1.564(6)	C(8)–C(15)	1.545(6)
C(21)–C(22)	1.539(6)	C(15)–C(18)	1.556(6)
C(22)–C(45)	1.554(7)	C(18)–C(19)	1.545(7)
C(11)–C(17)	1.528(7)	C(8)–C(28)	1.511(7)
C(11)–C(12)	1.513(6)	C(8)–C(40)	1.556(6)
C(14)–C(45)	1.546(6)	C(16)–C(19)	1.528(6)
C(32)–C(45)	1.540(7)	C(13)–C(19)	1.519(7)
C(17)–C(25)	1.366(7)	C(28)–C(33)	1.391(7)
C(12)–C(31)	1.386(7)	C(35)–C(40)	1.391(7)
C(14)–C(51)	1.385(8)	C(16)–C(38)	1.400(8)
C(32)–C(37)	1.384(8)	C(13)–C(47)	1.393(7)
Angles (°)			
Bond angles			
C(11)–C(21)–C(22)	117.4(3)	C(8)–C(15)–C(18)	117.4(4)
C(21)–C(22)–C(45)	116.8(4)	C(15)–C(18)–C(19)	117.1(4)
C(17)–C(11)–C(21)	111.1(4)	C(15)–C(8)–C(28)	111.6(4)
C(12)–C(11)–C(21)	113.2(4)	C(15)–C(8)–C(40)	111.6(4)
C(14)–C(45)–C(22)	112.5(4)	C(16)–C(19)–C(18)	111.8(4)
C(22)–C(45)–C(32)	111.3(4)	C(13)–C(19)–C(18)	112.3(4)
O(5)–C(11)–C(12)	105.8(4)	O(9)–C(8)–C(40)	105.3(4)
O(6)–C(45)–C(14)	109.5(4)	O(7)–C(19)–C(16)	108.4(4)
C(11)–C(17)–C(25)	121.2(4)	C(8)–C(28)–C(33)	121.8(4)
C(11)–C(12)–C(31)	118.7(4)	C(8)–C(40)–C(35)	115.9(4)
C(45)–C(14)–C(51)	117.6(4)	C(19)–C(16)–C(38)	117.6(4)
C(37)–C(32)–C(45)	119.8(4)	C(19)–C(13)–C(47)	121.5(5)
Torsion angles			
C(11)–C(21)–C(22)–C(45)	−102.1(5)	C(8)–C(15)–C(18)–C(19)	−100.6(5)
C(17)–C(11)–C(21)–C(22)	−59.5(4)	C(28)–C(8)–C(15)–C(18)	−61.2(4)
C(12)–C(11)–C(21)–C(22)	176.1(5)	C(40)–C(8)–C(15)–C(18)	176.0(5)
C(21)–C(22)–C(45)–C(14)	175.2(5)	C(15)–C(18)–C(19)–C(16)	174.2(6)
C(21)–C(22)–C(45)–C(32)	−60.4(4)	C(15)–C(18)–C(19)–C(13)	−59.7(4)
C(21)–C(11)–C(17)–C(25)	−85.5(5)	C(15)–C(8)–C(28)–C(33)	−81.8(5)
C(21)–C(11)–C(12)–C(31)	−167.2(6)	C(15)–C(8)–C(40)–C(35)	−172.2(6)
C(51)–C(14)–C(45)–C(22)	−169.7(6)	C(38)–C(16)–C(19)–C(18)	−169.9(6)
C(37)–C(32)–C(45)–C(22)	102.8(6)	C(47)–C(13)–C(19)–C(18)	103.2(6)

Table 2. Selected bond lengths (Å) and angles (°) for (*R*)-**2**

Guest I[a]		Guest II[a,b]	MacroModel®/MM2*[b,c]
Bond lengths (Å)			
O(84)–C(78)	1.204(11)	1.195(11)	1.211
C(70)–C(78)	1.531(9)	1.493(9)	1.524
C(70)–C(90)	1.509(9)	1.520(9)	1.540
C(74)–C(90)	1.525(10)	1.516(10)	1.512
C(64)–C(74)	1.383(10)	1.386(11)	1.398
Angles (°)			
Bond angles			
C(78)–C(70)–C(90)	114.8(6)	113.0(6)	112.3
C(70)–C(90)–C(74)	114.1(6)	114.1(6)	112.5
C(90)–C(74)–C(99)	121.7(7)	121.3(7)	121.0
Torsion angles			
C(78)–C(70)–C(90)–C(74)	−174.9(9)	−174.4(9)	−175.3
C(64)–C(74)–C(90)–C(70)	71.5(7)	67.2(7)	76.7

[a] Obtained by the X-ray crystallography.
[b] Geometrical parameters listed were corresponded to that for guest I.
[c] Obtained by MacroModel®/MM2* conformational search.

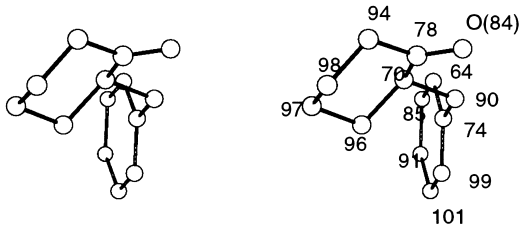

Figure 2. Stereoview of the most stable conformation of (*R*)-**2** obtained by MacroModel®/MM2*. Numbering for atoms was conformed to atomic numbers assigned to guest I by the X-ray crystallography.

that the conformation of the guest I resembles that of the guest II and the most stable one obtained by the calculation. However, a careful comparison between the X-ray and the calculation results (see the torsion angle C(64)–C(74)–C(90)–C(70) in Table 2) reveals that the induced-fit phenomena of a guest molecule into the cavity is caused by twisting of the phenyl group.

2.2. Crystal structure of the complex 1·(*R*)-2

Several papers have reported that hydrogen bonds are one of the most important interactions between the host molecule **1** and various guest components in the inclusion complex.[10] In the present study, molecular association via hydrogen bonds is also observed. In fact, one hydroxy group (O5 or O9) on each of the host molecules interacts intramolecularly with another hydroxy group (O6 or O7), whose hydrogen is donated to the carbonyl oxygen on the guest. Thus, the host I and II are linked to the guest I and II with hydrogen bonds to form a set of host–guest complexes, respectively (see Fig. 1). Table 3 shows the geometric parameters of this hydrogen bonding.

As mentioned above, the asymmetric unit is constituted with two sets of the host–guest complex. And the unit cell is constructed with two sets of the asymmetric unit (Fig. 3). Fig. 4 illustrates the assembly of the complex **1**·(*R*)-**2**.

Table 3. Geometric parameters of hydrogen bonding

Host I and guest I		Host II and guest II	
Bond lengths (Å)			
O(5)–H(5)	0.715(3)	O(9)–H(9)	0.853(4)
O(6)–H(6)	0.727(3)	O(7)–H(7)	0.863(3)
Non-bonded distances (Å)			
O(5)···O(6)	2.697(5)	O(9)···O(7)	2.672(5)
H(5)···O(6)	2.038(3)	H(9)···O(7)	1.821(3)
O(6)···O(84)[a]	2.705(7)	O(7)···O(80)[b]	2.672(5)
H(6)···O(84)[a]	2.076(7)	H(7)···O(80)[b]	1.976(7)
Angles (°)			
Non-bonded angles			
O(5)–H(5)…O(6)	153.8(3)	O(9)–H(9)…O(7)	174.3(3)
O(6)–H(6)···O(84)[a]	145.2(3)	O(7)–H(7)···O(80)[b]	145.0(3)

Translation of symmetry code to equiv. pos. a=$x-1$, y, z; b=$x+1$, y, z.

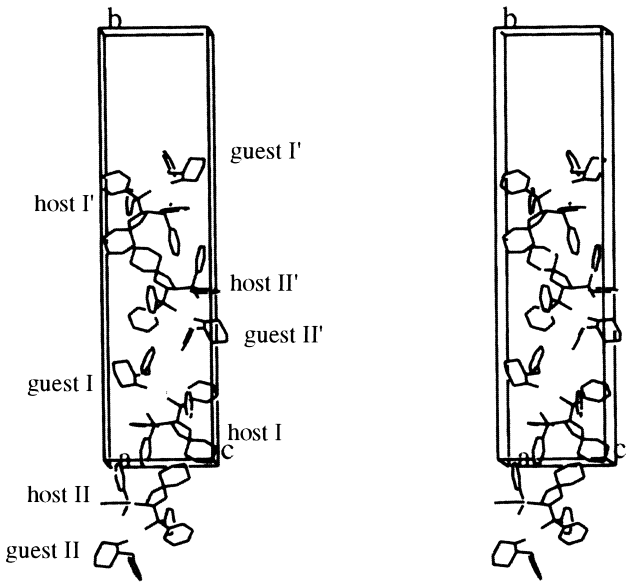

Figure 3. Stereoview of the crystal structure of the complex of **1**·(*R*)-**2** in a unit cell. Translation of symmetry code to equiv. pos. guest I=$x-1$, y, z; guest II=$x+1$, y, z; host I′ and host II′=$1-x$, $y+1/2$, $1-z$; guest I′=$2-x$, $y+1/2$, $1-z$; guest II′=$-x$, $y+1/2$, $1-z$.

Scrutiny of Fig. 4 reveals that van der Waals contacts between the hydrophobic groups stabilize the crystal packing as follows. (1) Host II′ (colored pink, blue, green, and red) self-assembles to form a layer owing to the interaction between the aromatic rings and the cyclohexyl ring. Selected interactions are shown in Fig. 5 with their distances. (2) Host I (colored black) and also host I′ (colored orange, yellowish green, and gray) aggregate with each other just like host II′. (3) A sophisticated gear-like connection between the gathering of host II′ and that of host I′ utilizing aromatic and cyclohexyl ring(s) is observed (see Fig. 4). Selected interactions are illustrated in Fig. 6 with their distances. (4) A guest II′ (colored yellow) connects zigzag to an adjacent guest II′ (colored dark yellow) via a guest I (colored blue) to form a bar (Fig. 7). Furthermore, the assembly of four host II′ molecules (colored pink, blue, green, and red) constitute a concave cavity in which the guest II′ (colored yellow) is accommodated via van der Waals contacts and the hydrogen bonding mentioned above (Fig. 8). Fig. 9 illustrates the selected van der Waals interactions between guest II′ (colored yellow) and host II′.

Thus, a sophisticated interaction with van der Waals contacts and the hydrogen bonding between host **1** and guest (*R*)-**2** stabilize the crystal packing. On the other hand, all attempts to obtain an inclusion complex of (*S*)-**2** and **1** were unsuccessful. This fact suggests that the chiral cavity constituted by the assembly of four host molecules accepts the (*R*)-isomer of **2** exclusively and the complex of **1**·(*R*)-**2** is more stable than the other. The present investigation assures us that the *thermodynamically controlled* deracemization is realized according to the concept mentioned in the introduction.

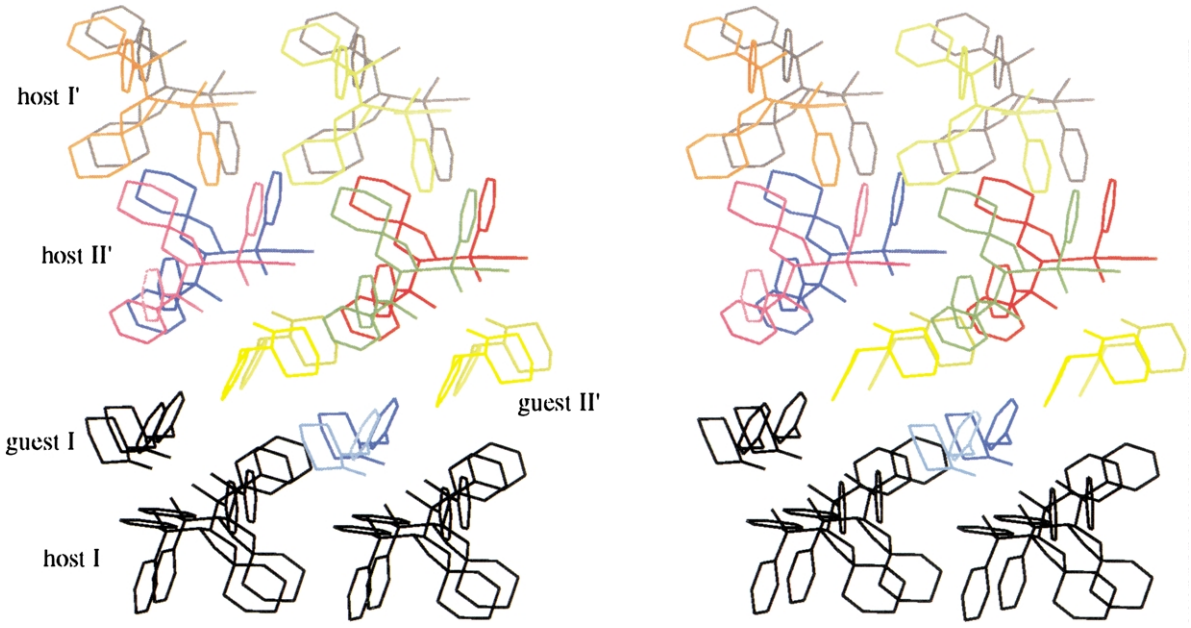

Figure 4. Stereoview of the assembly of the complex **1**·(*R*)-**2**. For clarity, host II, guest II, and guest I′ in the unit cell are omitted.

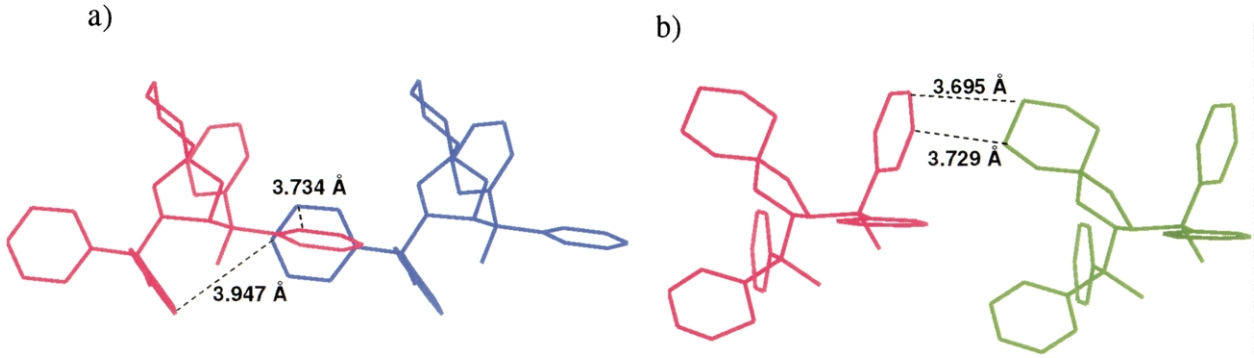

Figure 5. Selected van der Waals interactions between host II′. (a) View from a–b plane of the assembling host II′. (b) View from b–c plane of the assembling host II′. Symmetry code; host II′ (colored pink)=$-x$, $y+1/2$, $-z$; host II′ (colored blue)=$1-x$, $y+1/2$, $-z$; host II′ (colored green)=$-x$, $y+1/2$, $1-z$.

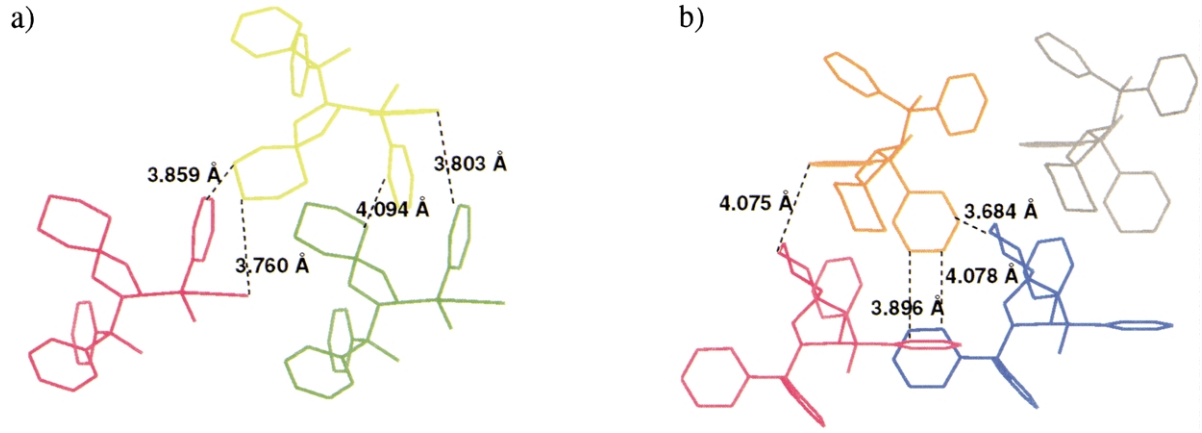

Figure 6. Selected van der Waals interactions between host II′ and host I′. (a) View from b–c plane of the assembling host II′ and host I′. (b) View from a–b plane of the assembling host II′ and host I′. Symmetry code; host II′ (colored pink) and host I′ (colored orange)=$-x$, $y+1/2$, $-z$; host II′ (colored green) and host I′ (yellow green)=$-x$, $y+1/2$, $1-z$; host II′ (colored blue) and host I′ (colored gray)=$1-x$, $y+1/2$, $-z$.

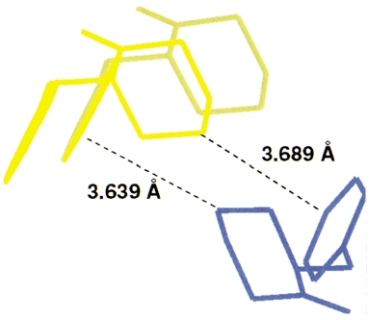

Figure 7. Selected van der Waals interactions between guest II′–guest I–guest II′. View from b–c plane of the assembling guest II′ and guest I. Symmetry code; guest I (colored blue)=x, y, z; guest II′ (colored yellow)=$-x$, $y+1/2$, $-z$; guest II′ (colored dark yellow)=$1-x$, $y+1/2$, $-z$.

3. Experimental

3.1. Preparation of the 1·(*R*)-2 complex

To a suspension of (*R*)-**2** (62% ee,[11] 500 mg, 2.66 mmol) and **1** (1.35 g, 2.66 mmol) in petroleum ether (1 mL) was added ether (about 4–5 mL) until the mixture became a clear solution. When the solution was kept at rt for a few days, a 1:1 inclusion complex of **1** and (*R*)-**2** of 96% ee was obtained as colorless prisms (532 mg, 29%), from which a suitable single crystal was selected.

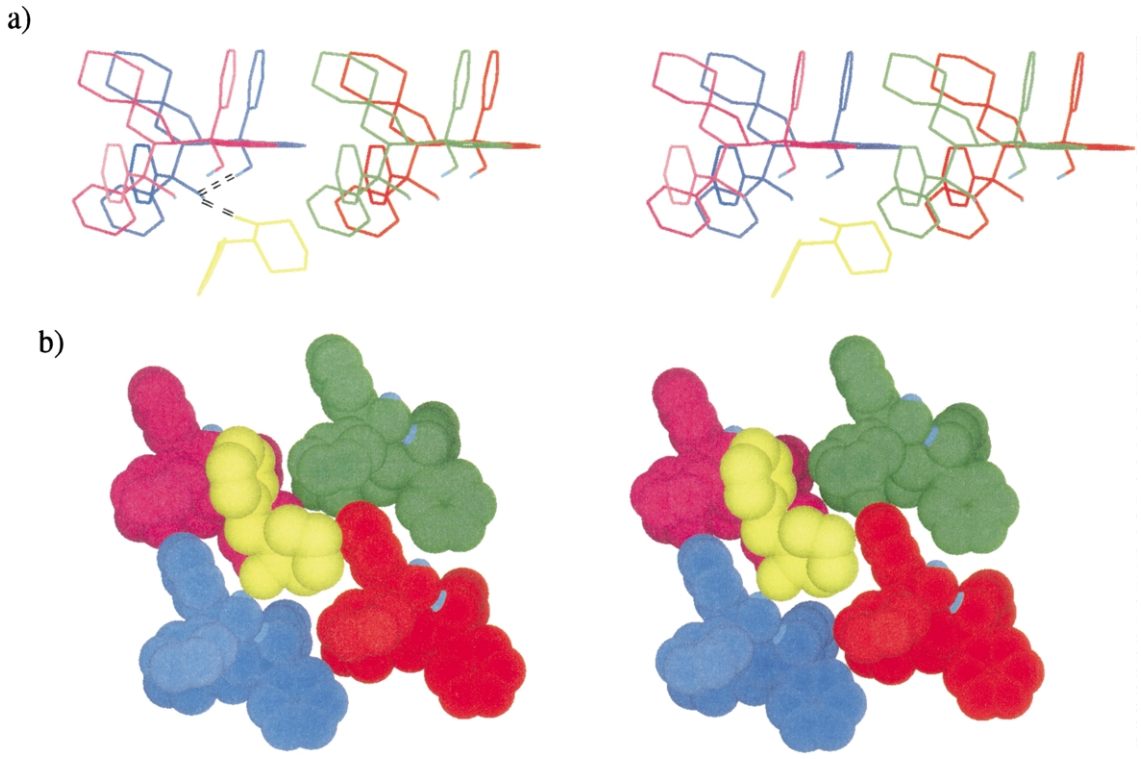

Figure 8. Stereoview of the accommodation of guest II′ in the cavity constituted by the aggregation of host II′. Symmetry code; host II′ (colored pink) and guest II′ (colored yellow)=$-x$, $y+1/2$, $-z$; host II′ (colored blue)=$1-x$, $y+1/2$, $-z$; host II′ (colored green)=$-x$, $y+1/2$, $1-z$; host II′ (colored red)=$1-x$, $y+1/2$, $1-z$. (a) View from b–c plane. Hydrogen bond between host and guest is represented by double dashed lines. (b) View from a–c plane denoted by space-filling representation.

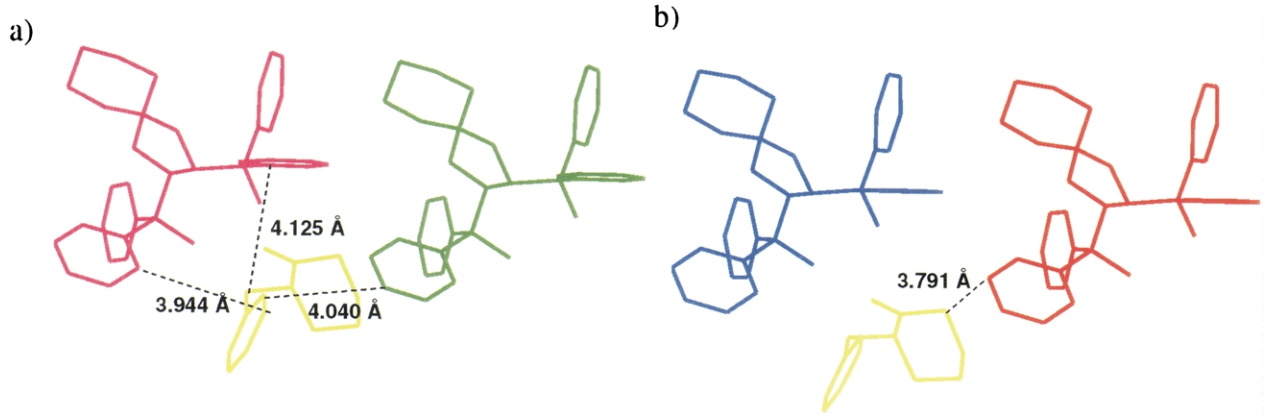

Figure 9. Selected van der Waals interactions between guest II′ and host II′. (a) View from b–c plane of the assembling guest II′ and host II′. (b) View from b–c plane of the assembling guest II′ and host II′. Symmetry code; host II′ (colored pink) and guest II′ (colored yellow)=$-x$, $y+1/2$, $-z$; host II′ (colored blue)=$1-x$, $y+1/2$, $-z$; host II′ (colored green)=$-x$, $y+1/2$, $1-z$; host II′ (colored red)=$1-x$, $y+1/2$, $1-z$.

Table 4. Crystal data and experimental conditions

Chemical formula/formula weight	$2(C_{34}H_{34}O)\cdot 2(C_{13}H_{16}O)$/ 1389.82
Crystal system/space group	Monoclinic/$P2_1$
Z	2
a, b, c (Å)	9.613(5), 40.077(9), 9.976(4)
β (°)	90.94(4)
V (Å^3)	3843.0(3)
D_x (Mg m^{-3})	1.201
Diffractometer	MXC18
Radiation	Cu Kα
λ (Å)	1.54178
μ (Cu Kα) (mm^{-1})	0.60
Crystal description/crystal dimensions (mm^3)	Cube/0.35×0.3×0.2
T (K)	298
$2\theta_{max}$ (°)	126.94
Range of h, k and l	$-11\leq h\leq 10$, $-45\leq k\leq 32$, $-11\leq l\leq 0$
Reflections: independent/ observed	6454/4783
$R(F)(I>3\sigma(I))$/ $wR(F^2)(I>3\sigma(I))$	0.043/0.088
S	1.101
Extinction coefficient	None
$(\Delta/\sigma)^{max}$	0.018
$\Delta\rho$ (e Å^{-3})	−0.26, 0.28
Roger's η parameter	2.5(8)

3.2. X-Ray analyses

The 2:2 complex of 1·(*R*)-**2**, $(C_{34}H_{34}O_4)_2\cdot(C_{13}H_{16}O)_2$, FW=1389.82, crystallizes in a monoclinic system[12] of the space group $P2_1$ with **2** compositions of 2:2 complex in a unit cell. The crystal data and the experimental details are summarized in Table 4. The structure of the **1**·(*R*)-**2** complex was solved by the direct method with the program SIR97.[13] The structure was refined by the full-matrix least squares method with the program maXus.[14] The weighting scheme was $w=1/(\sigma^2(F_o^2)+0.10000\times F_o^2)$ for the **1**·(*R*)-**2** complex. Positions of several hydrogen atoms were obtained on difference maps and those of the others were calculated geometrically. The anisotropic and isotropic temperature factors were applied to non-hydrogen atoms and hydrogen atoms in the final refinement, respectively. The positional parameters of the hydrogen atoms were constrained to have the C–H distances of 0.96 Å. Atomic scattering factors were taken from the International Tables for Crystallography.[15] Crystallographic data (excluding structure factors) for the structures in this paper have been deposited with the Cambridge Crystallographic Data Centre as supplementary publication numbers CCDC 179876. Copies of the data can be obtained, free of charge, on application to CCDC, 12 Union Road, Cambridge, CB2 1EZ, UK [fax: +44(0)-1223-336033 or e-mail: deposit@ccdc.cam.ac.uk].

Acknowledgements

This work was partially supported by a Grant-in-Aid for Encouragement of Young Scientists from the Ministry of Education, Science, Sports, and Culture of Japan.

References

1. Tsunoda, T.; Kaku, H.; Nagaku, M.; Okuyama, E. *Tetrahedron Lett.* **1997**, *38*, 7759–7760 and references cited therein.
2. Kaku, H.; Ozako, S.; Kawamura, S.; Takatsu, S.; Ishii, M.; Tsunoda, T. *Heterocycles* **2001**, *55*, 847–850.
3. Seebach, D.; Beck, A. K.; Imwinkelried, R.; Roggo, S.; Wonnacott, A. *Helv. Chem. Acta* **1987**, *70*, 954–974.
4. Seebach, D.; Beck, A. K.; Heckel, A. *Angew. Chem., Int. Ed. Engl.* **2001**, *40*, 92–138 and references cited therein.
5. Chang, G.; Guida, W. C.; Still, W. C. *J. Am. Chem. Soc.* **1989**, *111*, 4379–4386.
6. MacroModel® V6.5, Schrödinger Inc. was used.
7. Mohamadi, F.; Richards, N. G. J.; Guida, W. C.; Liskamp, R.; Lipton, M.; Caufield, C.; Chang, G.; Hendrickson, T.; Still, W. C. *J. Comput. Chem.* **1990**, *11*, 440–467.
8. Still, W. C.; Tempczyk, A.; Hawley, R. C.; Hendrickson, T. *J. Am. Chem. Soc.* **1990**, *112*, 6127–6129.
9. Although the structure was also optimized in the GB/SA water solvent continuum model, there is no difference in either of them (in $CHCl_3$ or water).
10. (a) Olszewska, T.; Milewska, M. J.; Gdaniec, M.; Malçuszyńska, H.; Polçoński, T. *J. Org. Chem.* **2001**, *66*, 501. (b) Nishikawa, K.; Tsukada, H.; Abe, S.; Kishimoto, M.; Yasuoka, N. *Chirality* **1999**, *11*, 166. (c) Toda, F. *Comprehensive Supramolecular Chemistry*; MacNicol, D. D., Toda, F., Bishop, R., Eds.; Pergamon: Oxford, 1996; Vol. 6, p 465 and references cited therein.
11. The optical purity of **2** was determined by GLC analysis using a chiral column (SUPELCO α-DEX, 150°C). The absolute configuration was determined by $[\alpha]_D$ and CD spectrum. See: Meyers, A. I.; Williams, D. R.; Erickson, G. W.; White, S.; Druelinger, M. *J. Am. Chem. Soc.* **1981**, *103*, 3081–3087.
12. Subject to crystallization in an orthorhombic system, we reanalyzed the crystal structure of the complex. However, the calculation gave no solution.
13. Altomare, A.; Burla, M. C.; Camalli, M.; Cascarano, G. L.; Giacovazzo, C.; Guagliardi, A.; Moliterni, A. G. G.; Spagna, R. *J. Appl. Crystallogr.* **1999**, *32*, 115–119.
14. Mackay, S.; Gilmore, C. J.; Edwards, C.; Stewart, N.; Shankland, K. *maXus Computer Program for the Solution and Refinement of Crystal Structures*; Bruker Nonius, The Netherlands, MacScience, Japan and The University of Glasgow, 1999.
15. *International Tables for Crystallography*; Kynoch Press: Birmingham, 1974; Vol. IV.